Approximate thermodynamic structure for driven lattice gases in contact

Punyabrata Pradhan, Robert Ramsperger, and Udo Seifert
II. Institut für Theoretische Physik, Universität Stuttgart, Stuttgart D-70550, Germany
(Received 4 July 2011; published 6 October 2011)

For a class of nonequilibrium systems, called driven lattice gases, we study what happens when two systems are kept in contact and allowed to exchange particles with the total number of particles conserved. For both attractive and repulsive nearest-neighbor interactions among particles and for a wide range of parameter values, we find that, to a good approximation, one could define an intensive thermodynamic variable, such as the equilibrium chemical potential, that determines the final steady state for two initially separated driven lattice gases brought into contact. However, due to nontrivial contact dynamics, there are also observable deviations from this simple thermodynamic law. To illustrate the role of the contact dynamics, we study a variant of the zero-range process and discuss how the deviations could be explained by a modified large-deviation principle. We identify an additional contribution to the large-deviation function, which we call the excess chemical potential, for the variant of the zero-range process as well as the driven lattice gases. The excess chemical potential depends on the specifics of the contact dynamics and is in general *a priori* unknown. A contact dependence implies that, even though an intensive variable may equalize, the zeroth law could still be violated.

DOI: 10.1103/PhysRevE.84.041104 PACS number(s): 05.70.Ln, 05.20.−y

I. INTRODUCTION

Equilibrium systems, which satisfy detailed balance and therefore do not have any particle or energy current, are based on a well-founded thermodynamic theory. Studies of equilibrium systems start with the zeroth law, which is the cornerstone of equilibrium thermodynamics. The zeroth law states that, in equilibrium, there exists a set of intensive variables, each of which is conjugate to a corresponding extensive conserved quantity, and these intensive variables equalize when two systems are kept in contact and allowed to exchange the conserved quantities. Specifically, an equilibrium system in contact with a reservoir is characterized by the familiar Boltzmann distribution where the probability of a microstate C is given by $P(C) \sim \exp[-\beta\{H(C) - \mu N\}]$, with $H(C)$ the internal energy of configuration C, N the number of particles in the system, and the intensive variables β and μ the inverse temperature and the chemical potential of the reservoir, respectively. These variables β and μ are conjugate to the energy and particle number of the system. Moreover, in equilibrium, there is a class of general fluctuation-response relations, collectively called the fluctuation-dissipation theorem, which relates the response of a system upon the change of an intensive variable (e.g., chemical potential) to the fluctuation in the corresponding extensive variable (e.g., particle number).

One could inquire whether there can be a similar thermodynamic structure for nonequilibrium systems as well. Among the vast class of nonequilibrium systems, one ubiquitous subclass is that of systems having a nonequilibrium steady state (NESS) [1,2]. The systems in a NESS have time-independent macroscopic properties that are similar to those of systems in equilibrium. However, unlike in equilibrium, they have a steady current and generally cannot be characterized by the Boltzmann distributions with an *a priori* known energy functions. Perhaps not surprisingly, even for this conceptually simplest class of driven systems with a NESS, there is no well-founded thermodynamic structure. Intensive studies in this direction to find a suitable framework for the description of a NESS have been undertaken [1,3–7]. In this paper we ask whether a homogeneously driven many-particle system can be characterized in terms of an intensive thermodynamic variable that equalizes for two systems in contact. We address this question using a simple class of stochastic models called driven lattice gases.

Although there have been many attempts to define an intensive variable for driven systems in various specific contexts [8–11], there was no general formulation in this regard until recently when a prescription to define such a variable for driven systems was proposed by invoking a hypothesis called the asymptotic factorization property [12]. This property has been shown to be satisfied for a class of driven systems having short-range spatial correlations such as the zero-range process (ZRP).

The ZRP is one of the simplest examples of driven interacting many-particle systems that do not satisfy detailed balance and have nonequilibrium steady states [13]. Previously, the ZRP was mainly considered as a model system for various mass transport processes and was used to study the phenomenon of the condensation transition in nonequilibrium systems [14]. Recently, it was demonstrated [15] that the systems governed by the ZRP have a simple thermodynamic structure where a suitably defined intensive variable, such as the equilibrium chemical potential, indeed equalizes for two such systems in contact. There is also a corresponding fluctuation-response relation between the compressibility and the fluctuation in the particle number, which is satisfied exactly for a system in contact with a particle reservoir. The main advantage of studying these simple models such as the ZRP was that the steady-state probability distributions, which have simple factorized forms, can be calculated exactly and therefore various features of driven systems in contact can be studied analytically. Due to the simple form of the steady-state distribution, it was also possible to analyze the role of dynamics in the contact region between two systems.

However, for driven systems with nontrivial steady-state properties, the situation is expected to be far more complex. Here we consider a simple model of a driven interacting

many-particle system known as the Katz-Lebowitz-Spohn (KLS) model [16,17]. The KLS model, first introduced to study fast ionic conductors [18], is a paradigm in nonequilibrium statistical mechanics. The model describes a stochastic lattice gas of charged particles that is homogeneously driven by a constant externally applied electric field. Initially, the primary motivation behind studying the KLS model was to understand the nontrivial spatial structures and phase transitions in generic bulk-driven systems with nonequilibrium steady states. Since its introduction, the KLS model has been studied intensively. At present, the phase diagram in the plane of the temperature and electric-field strength is quite well known, mainly from extensive simulations [16,17,19,20] as well as the results from mean-field theory [21] and renormalization-group analysis of a continuum version of the model [20,22]. However, there is still no well-founded thermodynamic theory for these driven interacting many-particle systems.

In this paper we explore the equilibration between two driven lattice gases when they are brought into contact. Recently we studied the KLS model, with repulsive nearest-neighbor interactions among particles [23], which revealed a simple but approximate thermodynamic structure. Here we extend our previous studies to systems with attractive interactions as well. Interestingly, for both attractive and repulsive interactions and for a wide range of parameter values, we find that, to a very good approximation, there is an intensive thermodynamic variable, such as the equilibrium chemical potential, that determines the final steady state while two systems are allowed to exchange particles. Consequently, the zeroth law of thermodynamics and the fluctuation-response relation between the compressibility and the fluctuations in particle number are satisfied remarkably well in a wide range of parameter values.

There are, however, observable deviations from this simple thermodynamic structure, especially at high interaction strengths and large driving fields. We explain these deviations by expressing the asymptotic factorization property, which was initially proposed by Bertin *et al.* [12,15] and later discussed by us for driven lattice gases in Ref. [23], in a modified form where contributions to the large-deviation functions due to the contact dynamics are identified. To illustrate the origin of these deviations, we study the nontrivial role of the contact dynamics using first a simple variant of the ZRP and later the KLS model. We find that, depending on the various parameter values, the contact dynamics can amount to an excess chemical potential across the contact for the variant of the ZRP as well as the KLS model. This excess chemical potential is generally *a priori* unknown and in some sense arbitrary for an arbitrarily chosen contact dynamics. Therefore, it may not always be possible to assign to the individual systems an intensive variable that is independent of the contact between the two systems, thus accounting for the deviations from the zeroth law.

The paper is outlined as follows. In Sec. II we describe the model. In Sec. III we present the numerical results concerning the zeroth law for the KLS model and possible deviations from the law. In Sec. IV we discuss the excess chemical potential for a variant of the ZRP as well as a variant of the equilibrium KLS model. In Sec. V we describe how the large-deviation principle can be written in a modified form that can capture the deviations from the zeroth law and then discuss the excess chemical potential for the KLS model. We summarize in Sec. VI. In Appendix A we give a proof of the ansatz for the steady-state probability distribution in the case of the ZRP. In Appendix B we discuss the fluctuation-response relation for the ZRP as well as for the KLS model.

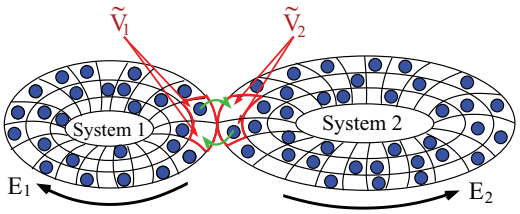

FIG. 1. (Color online) Schematic diagram of two nonequilibrium steady states in contact with the contact regions $\tilde{V}_1$ and $\tilde{V}_2$. Particles are allowed to be exchanged through the contact regions $\tilde{V}_1$ and $\tilde{V}_2$. In this process the total number of particles $N = N_1 + N_2$ is conserved, where N_1 and N_2 are the number of particles in systems 1 and 2, respectively.

II. MODEL

We consider stochastic lattice gases of charged particles that are driven out of equilibrium by constant externally applied electric fields in the bulk and therefore have spatially homogeneous steady states [16]. Particles move on a discrete lattice and jump stochastically from one site to any of its nearest-neighbor sites, preferably in the direction of the external driving field of magnitude E. Due to hard-core repulsion among particles, a lattice site can be occupied by at most one particle. In addition, particles may also interact with each other through a nearest-neighbor pair potential of interaction strength K. We define the occupation variable $\eta(\mathbf{r})$ at a site $\mathbf{r} \equiv \{r_x, r_y\}$, where $\eta(\mathbf{r}) = 0,1$: If a site $\mathbf{r}$ is occupied, $\eta(\mathbf{r}) = 1$; otherwise $\eta(\mathbf{r}) = 0$. We consider two systems of lattice gases where systems 1 and 2 are confined, respectively, in volume V_1 and volume V_2 (see Fig. 1). When two such systems are brought into contact, they are connected at a finite set of points V_1' and V_2', which are subsets of V_1 and V_2, respectively ($V_1', V_2' \ll V_1, V_2$), and while in contact they can exchange particles with each other. The energy function H of the two systems, combined, is given by

$$H = K_1 \sum_{\langle \mathbf{r}_1, \mathbf{r}_1' \rangle} \eta(\mathbf{r}_1)\eta(\mathbf{r}_1') + K_2 \sum_{\langle \mathbf{r}_2, \mathbf{r}_2' \rangle} \eta(\mathbf{r}_2)\eta(\mathbf{r}_2'), \qquad (1)$$

where $\langle , \rangle$ denotes sum over nearest-neighbor sites with $\mathbf{r}_1, \mathbf{r}_1' \in V_1$ and $\mathbf{r}_2, \mathbf{r}_2' \in V_2$ and K_1 and K_2 are the strengths of interactions among particles for the respective systems. Note that systems may in general have different microscopic dynamics depending on the interaction strengths K_1 and K_2. Constant driving fields E_1 and E_2 in systems 1 and 2, respectively, are applied in the x direction, with periodic boundary conditions imposed in both the x and y directions.

We choose jump rates of particles such that they satisfy the local detailed balance condition [16]. A pair of nearest-neighbor sites located at $\mathbf{r}$ and $\mathbf{r}'$ in a configuration C are chosen randomly and an attempt is made to interchange the occupation variables where the attempted final configuration is denoted by C'. Let us denote the corresponding transition

rate from configuration C to C' as $w(C'|C)$. For movements of particles inside the same system (i.e., particles not jumping from one system to the other), a quantity $\Delta(E) = H(C') - H(C) - E(r'_x - r_x)$, which depends on the driving field E, is defined, where r_x denotes the x component of the position vector $\mathbf{r}$ and $H(C)$ is the energy of the configuration C. The transition rate is assigned to be

$$w(C'|C) = \min\{1, e^{-\beta\Delta(E)}\}, \tag{2}$$

where β is the inverse temperature of the heat bath. When the chosen pair of sites is such that a jump is attempted from one system to the other across the contact, the transition rate is assigned to be

$$w(C'|C) = \min\{1, e^{-\beta\Delta(0)}\}, \tag{3}$$

where $\Delta(0) = H(C') - H(C)$. Note that there is no field along the bonds connecting the two systems. In the simulations we consider two-dimensional systems ($V = L \times L$) with periodic boundaries in both directions. We set $\beta = 1$ throughout the paper.

When $E_1 = E_2 = 0$ the jump rates satisfy the detailed balance condition and the configuration C of the combined system has the Boltzmann probability distribution $P(C) \sim \exp[-H(C)]$. For $E_1, E_2 \neq 0$ there is a constant current in the steady state. However, unlike in equilibrium, the nonequilibrium steady-state probability distribution generally is not given by the Boltzmann distribution with an *a priori* known energy function and, except for a few cases (e.g., with only hard-core interactions), the steady-state probability distribution is not known. When two systems are brought into contact, they can exchange particles with the total number of particles $N = N_1 + N_2$ conserved, where $N_1 = \sum_{\mathbf{r}_1 \in V_1} \eta(\mathbf{r}_1)$ and $N_2 = \sum_{\mathbf{r}_2 \in V_2} \eta(\mathbf{r}_2)$ are the numbers of particles in systems 1 and 2, respectively. In the following sections we consider the cases in which the conserved quantity is the number of particles and therefore attempt to define an intensive variable, called the chemical potential in analogy with equilibrium, which is conjugate to the conserved particle number.

Bilayer systems have been considered before in which particles can jump from one layer to the other at any site in the cases of driven [24] and equilibrium [25] layers in contact. Here, however, we consider the case in which particles can jump from one system to the other through a very small contact region between the systems. Moreover, these previous studies have mainly focused on the phase transition from the disordered state with a fluid phase to the ordered symmetry-broken state with coexisting phases of gas and liquid and on properties of droplets that are formed in the coexisting phases. In this paper we confine ourselves to only the disordered fluid phase that is obtained by suitably choosing the interaction strengths K_1 and K_2 and the driving fields E_1 and E_2. Although the model considered here is very simple, the chosen transition rates can be physically motivated through the local detailed balance condition and therefore the model could still capture, in a crude way, the features of more realistic systems.

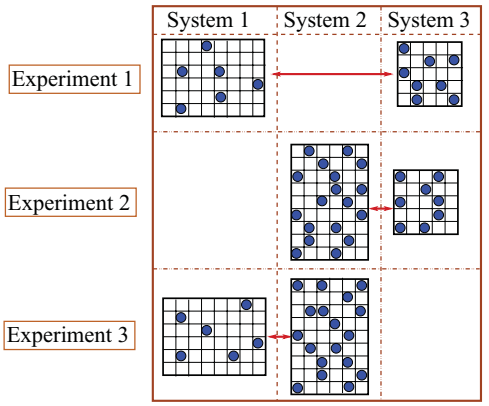

FIG. 2. (Color online) Schematic diagram to test the zeroth law of thermodynamics for equilibrium systems using a sequence of three thought experiments where three systems (for simplicity, shown in two dimensions) are separately kept in contact with each other and allowed to equilibrate. In experiment 1, systems 1 and 3 are in contact. In experiment 2, systems 2 and 3 are in contact. In experiment 3, systems 1 and 2 are in contact.

III. NUMERICAL RESULTS

A. Zeroth law

First let us describe the zeroth law in the context of equilibrium systems. We consider three systems and perform the following three thought experiments, which are schematically presented in Fig. 2 . In the first experiment systems 1 and 3 are brought into contact and allowed to exchange particles with each other. Systems 1 and 3 eventually equilibrate and reach a final equilibrium state with constant average densities n_1 and n_3, respectively. In the second experiment systems 2 and 3 are separately brought into contact and allowed to exchange particles. In this case the initial density of system 2 is tuned such that system 3 has the same final density as that of system 3 in the first experiment. Let us denote the final equilibrium densities for systems 2 and 3 in the second experiment as n_2 and n_3, respectively. Now in the third experiment systems 1 and 2 with initial densities n_1 and n_2, respectively, are brought into contact and allowed to exchange particles. One could ask what the final densities in this case would be. The zeroth law of thermodynamics provides the answer that the final densities will not change anymore and will be exactly equal to the respective initial densities. Thus the zeroth law allows us to assign to an equilibrium system an intensive thermodynamic variable, called the chemical potential, that equalizes for two systems in contact. Note that, in Fig. 2, if one compares the density profiles of two systems in the same column, the corresponding average density profiles would be exactly the same.

We use the preceding strategy to test the zeroth law for systems in nonequilibrium steady states. We perform the same set of numerical experiments as described above, but now with two of the systems driven out of equilibrium due to external driving fields present in the bulk of the individual systems. Interestingly, similar to the equilibrium case, we observe that, for various values of interaction strengths, driving fields, and densities, the zeroth law is quite well satisfied, i.e., if two driven lattice gases are separately equilibrated with a common

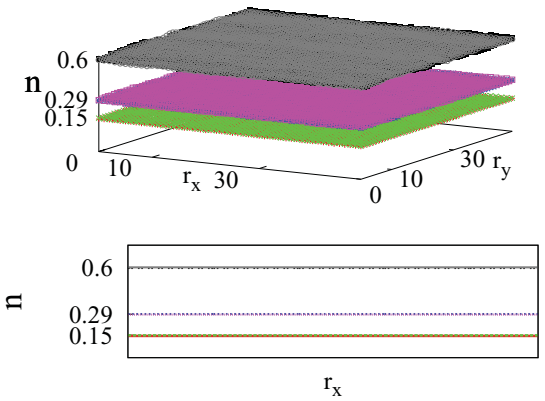

FIG. 3. (Color online) Numerical experiments to test the zeroth law (2×2 contact region). The top panel shows the average densities as a function of position coordinates r_x and r_y. The bottom panel shows the cross sections (in the x direction) of the density profiles. For driven system 1, $K = -1$ and $E = 6$ (top density profiles); for driven system 2, $K = -0.75$ and $E = 4$ (middle density profiles); for equilibrium system 3, $K = 0$ and $E = 0$ (bottom density profiles). All systems considered here are with same volume $V = 50 \times 50$. In experiment 1, system 1 with density $n_1 \simeq 0.60$ (top gray profile in the top panel or top dashed gray line in the bottom panel) equilibrated with system 3 with density $n_3 \simeq 0.15$ (bottom red profile in the top panel or bottom solid red line in the bottom panel). In experiment 2, system 2 with density $n_2 \simeq 0.29$ (middle magenta profile in the top panel or middle solid magenta line in the bottom panel) equilibrated with system 3 with density $n_3 \simeq 0.15$ (bottom green profile in the top panel or bottom dotted green line in the bottom panel). In experiment 3, system 1 with density n_1' (top black profile in the top panel or top dash-dotted black line in the bottom panel) equilibrated with system 2 with density n_2' (middle blue profile in the top panel or middle dotted blue line in the bottom panel), where $n_1' \simeq n_1$ and $n_2' \simeq n_2$.

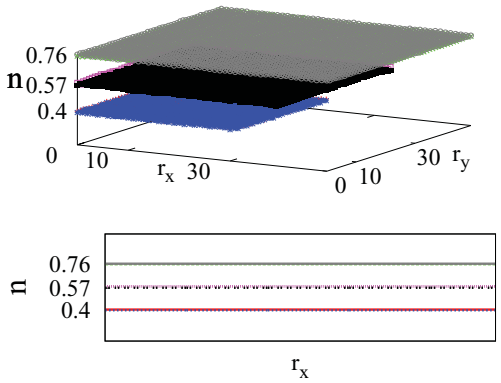

FIG. 4. (Color online) Numerical experiments to test the zeroth law (2×2 contact region). The top panel shows the average densities as a function of position coordinates r_x and r_y. The bottom panel shows the cross sections (in the x direction) of the density profiles. For driven system 1, $K = 3.75$, $E = 6$, and $V = 32 \times 32$ (bottom density profiles). For driven system 2, $K = 1.5$, $E = 5$, and $V = 40 \times 40$ (middle density profiles). For equilibrium system 3, $K = 0.75$, $E = 0$, and $V = 50 \times 50$ (top density profiles). In experiment 1, system 1 with density $n_1 \simeq 0.40$ (bottom red profile in the top panel or bottom solid red line in the bottom panel) equilibrated with system 3 with density $n_3 \simeq 0.76$ (top gray profile in the top panel or top dotted gray line in the bottom panel). In experiment 2, system 2 with density $n_2 \simeq 0.57$ (middle black profile in the top panel or middle dotted black line in the bottom panel) equilibrated with system 3 with density $n_3 \simeq 0.76$ (top green profile in the top panel or top solid green line in the bottom panel). In experiment 3, system 1 with density n_1' (bottom blue profile in the top panel or bottom dotted blue line in the bottom panel) equilibrated with system 2 with density n_2' (middle magenta profile in the top panel or middle solid magenta line in the bottom panel), where $n_1' \simeq n_1$ and $n_2' \simeq n_2$.

system with a fixed density, they will also equilibrate among themselves. Two such examples are given below where we choose a small 2×2 contact region.

1. Example of driven systems with attractive interactions

In Fig. 3 we consider three systems, a driven system 1 with $K = -1$, $E = 6$, a driven system 2 with $K = -0.75$, $E = 4$ and an equilibrium system 3 with $K = 0$, $E = 0$. First, system 1 with density $n_1 \simeq 0.60$ and system 2 with density $n_2 \simeq 0.29$ are separately equilibrated with system 3 with a fixed density $n_3 \simeq 0.15$. We then find that system 1 and system 2, with the initial densities $n_1 \simeq 0.60$ and $n_2 \simeq 0.29$ respectively, equilibrate with each other such that, to a very good approximation, the respective final steady-state values of densities $n_1' \simeq 0.60$ and $n_2' \simeq 0.29$ remain almost unchanged.

2. Example of driven systems with repulsive interactions

In Fig. 4 we consider three systems: a driven system 1 with $K = 3.75$ and $E = 6$, a driven system 2 with $K = 1.5$ and $E = 5$, and an equilibrium system 3 with $K = 0.75$ and $E = 0$. System 1 with density $n_1 \simeq 0.40$ and system 2 with density $n_2 \simeq 0.57$ are separately equilibrated with system 3 with a fixed density $n_3 \simeq 0.76$. In Fig. 4 one could see that systems 1 and 2 with the initial densities $n_1 \simeq 0.40$ and $n_2 \simeq 0.57$, respectively, equilibrate with each other with their respective final densities $n_1' \simeq 0.39$ and $n_2' \simeq 0.58$. Also in this case the zeroth law is satisfied to a good approximation, where final densities n_1' and n_2' remain almost the same as the initial densities.

Interestingly, as seen in Figs. 3 and 4, two systems in contact have homogeneous density profiles even when one or both of them may be driven. The driven systems are indeed far away from equilibrium since the numerical values of the currents in the nonequilibrium steady states considered in Figs. 3 and 4 are near the respective maximum values of the currents (data not shown). Moreover, in the top panel of Fig. 4, system 1 with density $n_1 \simeq 0.40$ has a homogeneous disordered state in contrast to an ordered state for the corresponding equilibrium system. The equilibrium system, with the same interaction strength $K = 3.75$ and the same density, has a symmetry-broken ordered phase with a checkerboardlike pattern where sublattice densities are different [17].

Importantly, the macroscopic properties such as densities do indeed depend on the driving field when a driven system 1 is kept in contact with an equilibrium system 2 with a fixed density n_2. This can be seen in the behavior of density n_1 of a driven system as a function of driving field E_1. We consider the driven systems that were previously used to test the zeroth law in Figs. 3 and 4. In the top panel of Fig. 5, densities of two driven systems with attractive interactions, with $K_1 = -1$

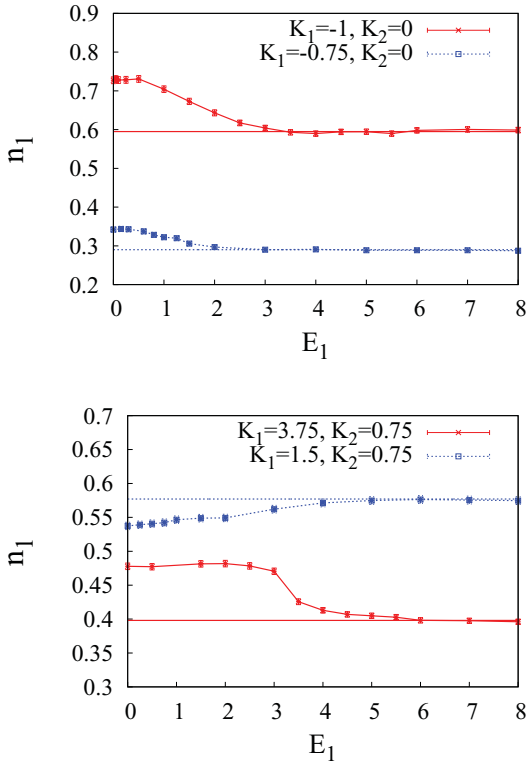

FIG. 5. (Color online) Density n_1 of a driven system 1 as a function of driving field E_1 when system 1 is in contact (in the 2×2 contact region) with equilibrium system 2 with a fixed density n_2. The top panel shows the densities of two driven systems with interaction strengths $K_1 = -1$ and -0.75 plotted as a function of their respective driving fields E_1 when the systems are separately in contact with an equilibrium system with $K_2 = 0$ and $n_2 \simeq 0.15$. The bottom panel shows the densities of two driven systems with interaction strengths $K_1 = 3.75$ and 1.5 plotted as a function of their respective driving fields E_1 when the systems are separately in contact with an equilibrium system with $K_2 = 0.75$ and $n_2 \simeq 0.76$. Horizontal straight lines are guides to the eye, representing the density values of the corresponding driven systems at very large driving fields.

and -0.75, have been plotted as a function of the driving fields E_1 in their respective systems where both systems are separately kept in contact with an equilibrium system with $K_2 = 0$ and a fixed density $n_2 \simeq 0.15$. In the bottom panel of Fig. 5, densities of two other driven systems with repulsive interactions, with $K_1 = 3.75$ and 1.5, have been plotted as a function of the driving fields E_1 in their respective systems where both systems are now separately kept in contact with an equilibrium system with $K_2 = 0.75$ and a fixed density $n_2 \simeq 0.76$. One could see that the densities vary quite significantly, by almost 10% or more from the respective equilibrium values depending on the interaction strengths, when the driving field varies from $E_1 = 0$ to a large value $E_1 \gg K_1$.

Provided that the zeroth law is satisfied, one can define a chemical potential even for a driven system as follows. A driven system is kept in contact with an equilibrium system and allowed to reach a steady state. Then, in the steady state, one can simply assign the chemical potential of the equilibrium system to the driven one. For nonzero interaction strengths $K \neq 0$, even the equilibrium chemical potential μ cannot be

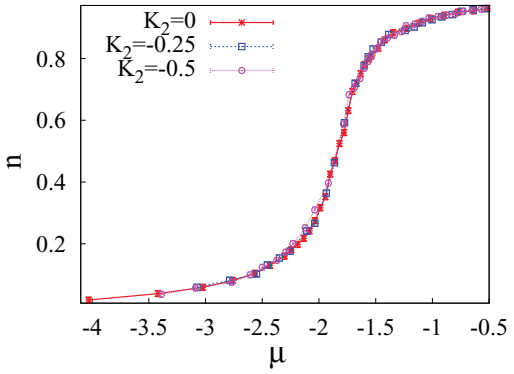

FIG. 6. (Color online) Density n vs chemical potential μ plotted for a driven system with $K_1 = -1$ and $E_1 = 6$, which is separately kept in contact (in the 2×2 contact region) with three equilibrium systems with interaction strengths $K_2 = 0$ (asterisks), -0.25 (squares), and -0.5 (circles). The collapse of the curves agrees well with the zeroth law.

calculated directly as one does not know the explicit form of $\mu(n)$ as a function of density n. However, for an equilibrium system with noninteracting hard-core particles $K = 0$, the chemical potential μ can be expressed as a function of density n, where

$$\mu = \ln\left(\frac{n}{1-n}\right), \tag{4}$$

by using the relation $\mu = -(\partial s/\partial n)$, where $s = -[n \ln n + (1-n)\ln(1-n)]$ is the equilibrium entropy per lattice site. Since the zeroth law is exactly satisfied in equilibrium, the chemical potential for any equilibrium system with $K \neq 0$ can be measured by keeping the system in contact with an equilibrium system with $K = 0$ and then assigning a chemical potential for a system with $K = 0$ to that with $K \neq 0$. In Fig. 6 we plot the density n as a function of chemical potential μ when a driven system with $K_1 = -1$ and $E_1 = 6$ is separately kept in contact with three equilibrium systems with various interaction strengths $K_2 = 0$, -0.25, and -0.5. Given that the zeroth law is satisfied, the various curves for density as a function of chemical potential should fall on each other. The collapse of curves in Fig. 6 indeed agrees quite well with the zeroth law.

We have studied the dependence of densities on the system sizes as well. We find that the densities of two systems in contact with each other, when one or both systems may be driven, are almost independent of system sizes. In Fig. 7 we plot the density n as a function of chemical potential μ for various system sizes and for various values of interaction strengths and driving fields. The densities seem to depend only on the interaction strengths and driving fields of their respective systems.

In Figs. 3 and 4 we have tested the zeroth law for only a particular set of values of densities. We now study the zeroth law for other various densities where the interaction strengths and driving fields are kept fixed. We consider driven systems 1 and 2 with respective densities n_1 and n_2, where the systems are separately equilibrated with an equilibrium system 3 with density n_3 and corresponding chemical potential μ. Then systems 1 and 2, with the respective initial densities n_1

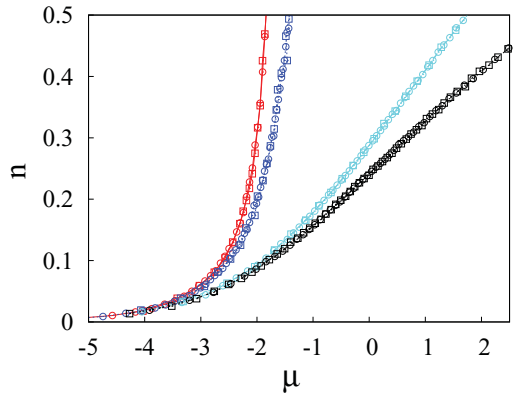

FIG. 7. (Color online) Density n as a function of chemical potential μ for driven systems (with fixed K_1 and E_1) with different values of system size V_1 in contact (in the 2×2 contact region) with an equilibrium system of noninteracting hard-core particles (with $K_2 = 0$ and $E_2 = 0$) with different values of system size V_2. Circles correspond to the case in which system 1, with $V_1 = 32 \times 32$, is in contact with system 2, with $V_2 = 32 \times 32$. Squares correspond to the case in which system 1, with $V_1 = 20 \times 20$, is in contact with system 2, with $V_2 = 100 \times 100$. Shown from left to right are two curves [red (leftmost)] for systems with $K_1 = -1$ and $E_1 = 6$, two curves [blue (second from left)] for systems with $K_1 = -0.75$ and $E_1 = 4$, two curves [sky blue (third from left)] for systems with $K_1 = 1$ and $E_1 = 6$, and two curves [black (rightmost)] for systems with $K_1 = 2$ and $E_1 = 2$.

and n_2, are equilibrated with each other where they eventually reach final densities n_1' and n_2'. Clearly, if the zeroth law is satisfied, then the corresponding initial and final densities would be exactly the same, i.e., $n_1 = n_1'$ and $n_2 = n_2'$. We consider the systems as previously discussed in Figs. 3 and 4. In Fig. 8 we plot n_1 and n_1' for system 1 with $K = -1$ and $E = 6$ as well as n_2 and n_2' for system 2 with $K = -0.75$

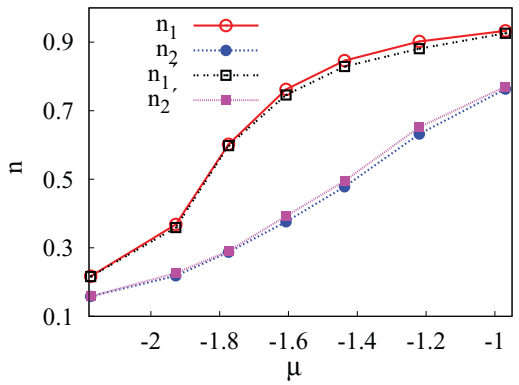

FIG. 8. (Color online) Final densities n_1' (open black squares) and n_2' (solid magenta squares) for two driven systems (with $K = -1$ and $E = 6$ and with $K = -0.75$ and $E = 4$, respectively) in contact (in the 2×2 contact region) with each other, compared with their respective initial densities n_1 (open red circles) and n_2 (solid blue circles). The initial densities correspond to those obtained by keeping the driven systems separately in contact (in the 2×2 contact region) with an equilibrium system of a fixed chemical potential μ. If the zeroth law is satisfied, the initial and final densities should be exactly the same for a given μ.

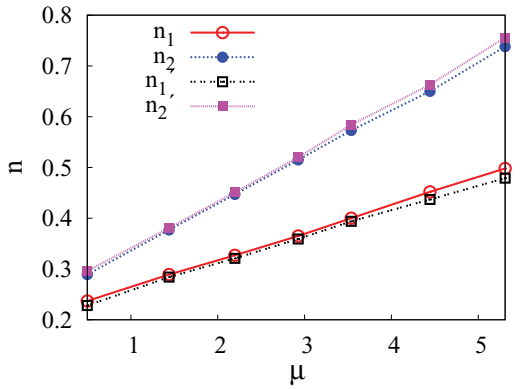

FIG. 9. (Color online) Final densities n_1' (open black squares) and n_2' (solid magenta squares) for two driven systems (with $K = 3.75$ and $E = 6$ and with $K = 1.5$ and $E = 5$, respectively) in contact (in the 2×2 contact region) with each other, compared with their respective initial densities n_1 (open red circles) and n_2 (solid blue circles). The initial densities correspond to those obtained by keeping the driven systems separately in contact (in the 2×2 contact region) with an equilibrium system of a fixed chemical potential μ. If the zeroth law is satisfied, the initial and final densities should be exactly the same for a given μ.

and $E = 4$ as a function of chemical potential μ of the equilibrium system 3, with $K = E = 0$. Similarly, in Fig. 9 we plot n_1 and n_1' for system 1 with $K = 3.75$ and $E = 6$ as well as n_2 and n_2' for system 2 with $K = 1.5$ and $E = 5$ as a function of chemical potential μ of the system 3, with $K = 0.75$ and $E = 0$. Although the zeroth law is satisfied to a good approximation, there are indeed small but observable deviations from the law, i.e., up to 5% deviations in the final densities from the corresponding initial density values. In the following section we discuss the deviations from the zeroth law in more detail.

B. Deviations from the zeroth law

In the preceding section we have seen that, for a large parameter range, the driven lattice gases have an approximate but remarkably simple thermodynamic structure. However, it should be noted that there are also larger observable deviations from the simple thermodynamic law, as discussed next.

In Fig. 10 we perform numerical experiments similar to that discussed before (see, e.g., Figs. 3 and 4) in which system 1 with density n_1 and system 2 with density n_2 are separately equilibrated with system 3 with a fixed density n_3. Then systems 1 and 2, with their respective initial densities n_1 and n_2, are equilibrated with each other where the final steady-state densities are n_1' and n_2', respectively. In the top, left panel of Fig. 10, six density profiles in the x direction are plotted for equilibrium systems 1, 2, and 3. As expected, for equilibrium systems, the zeroth law is exactly satisfied where $n_1 = n_1' \simeq 0.79$ (top density profiles) and $n_2 = n_2' \simeq 0.41$ (middle density profiles), i.e., initial densities are equal to their respective final densities. In the top, right panel of Fig. 10, six density profiles in the x direction are plotted when systems 1 and 3 are equilibrium systems but system 2 is driven with a large field $E_2 = 10$. In this case, the zeroth law is observed to be violated significantly where $n_1 \simeq 0.79 \neq n_1' \simeq 0.75$ (top

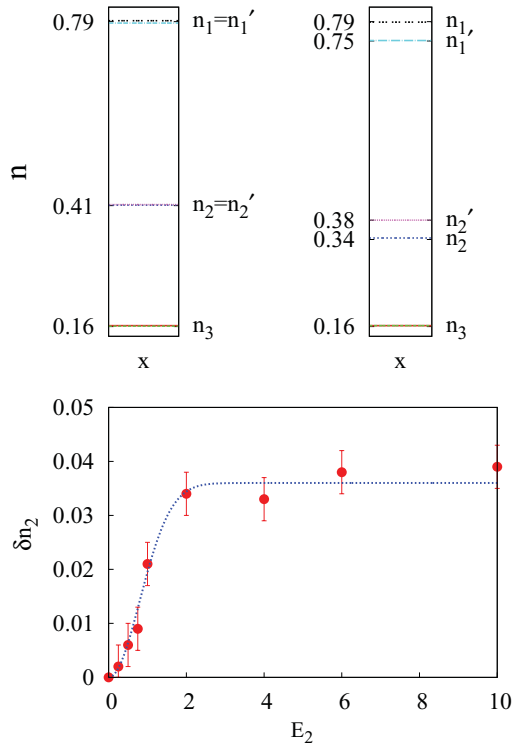

FIG. 10. (Color online) Cross sections (in the x direction) of the density profiles are plotted in top panel. Systems 1, 2, and 3 (all with the same size $V = 50 \times 50$ and 2×2 contact region) have interaction strengths $K = -1$ (top density profiles), -0.75 (middle density profiles), and 0 (bottom density profiles), respectively. First, system 1, with density n_1, and system 2, with density n_2, are separately equilibrated with system 3, with density n_3. Then systems 1 and 2, with initial densities n_1 and n_2, respectively, are equilibrated with each other where the final steady-state densities are n_1' and n_2', respectively. The top panel (left) shows equilibrium systems where $n_1 = n_1'$ and $n_2 = n_2'$. The top panel (right) shows system 2 driven with field $E_2 = 10$ where $n_1 \neq n_1'$ and $n_2 \neq n_2'$. The bottom panel shows the difference in density $\delta n_2 = n_2' - n_2$ plotted versus driving field E_2 for system 2. The blue line, which is a fitting function $a - be^{-\kappa E_2^2}$ with $a = 0.036$, $b = 0.036$, and $\kappa = 0.78$, is a guide to the eye.

density profiles) and $n_2 \simeq 0.34 \neq n_2' \simeq 0.38$ (middle density profiles), i.e., final densities change appreciably as compared to their respective initial densities. In the bottom panel of Fig. 10, the density difference $\delta n_2 = n_2' - n_2$ is plotted as a function of the driving field E_2 in system 2.

One can also observe the deviations from the zeroth law, which is now studied in a slightly different way as follows. We first try to assign a chemical potential to a driven system by keeping the system separately in contact with various equilibrium systems and then compare the density versus chemical potential curves. In Fig. 11 we plot the density n as a function of chemical potential μ for a driven system, with $K_1 = -1$ and $E_1 = 6$, which is separately kept in contact with three equilibrium systems with the following interaction strengths: $K_2 = 0$, -0.8, and -0.9. If the zeroth law was satisfied, all the curves should fall on each other. However, we observe that there are significant deviations that occur especially around the density $n = 1/2$. In Fig. 12 we plot n vs μ for another driven system, with repulsive interaction

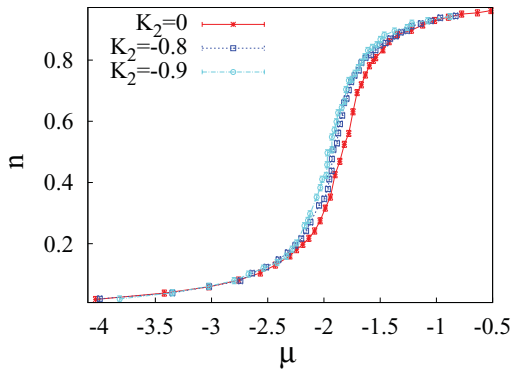

FIG. 11. (Color online) Density n as a function of chemical potential μ for a driven system with $K_1 = -1$ and $E_1 = 6$, which is separately kept in contact with three equilibrium systems with interaction strengths $K_2 = 0$, -0.8, and -0.9 (2×2 contact region).

$K_1 = 3.75$ and $E_1 = 6$, that is separately in contact with equilibrium systems with $K_2 = 0.75$ and 1. We again see deviations from the zeroth law when the density approaches $n = 1/2$.

IV. ROLE OF CONTACT DYNAMICS: EXACT RESULTS

A. Excess chemical potential in the ZRP

We now study a simple class of driven systems, known as the zero-range process [13], to understand the role of contact dynamics in the context of equalization of thermodynamic variables for driven systems. The ZRP is defined on a discrete lattice where, unlike the KLS model, there is no restriction on the occupation number of a site, i.e., the lattice sites can be occupied by more than one particle. The jump rate of a particle out of any site is assumed to depend on the number of particles on the site.

For simplicity, we consider two one-dimensional rings, ring 1 and ring 2, consisting of sites L_1 and L_2, respectively. The rings are kept in contact with each other so that they can exchange particles through the contact area. In the αth ring ($\alpha = 1,2$), any site i_α ($i_\alpha = 1,2,\ldots,L_\alpha$) is occupied with n_{i_α} particles. Any configuration C can be specified by using the

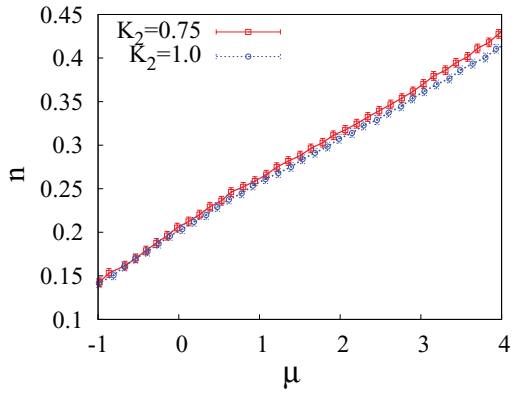

FIG. 12. (Color online) Density n as a function of chemical potential μ for a driven system with $K_1 = 3.75$ and $E_1 = 6$, which is separately kept in contact with two equilibrium systems with interaction strengths $K_2 = 0.75$ and 1 (2×2 contact region).

occupation numbers at all sites of two rings, $C \equiv (\{n_{i_1}\},\{n_{i_2}\})$. Two rings are connected at two sites, say, $i_1 = 1$ and $i_2 = 1$, through which particles can be exchanged between the rings. The dynamics is defined as follows: A particle at site i_α can jump only in one direction, say, to the nearest neighbor site $i_\alpha + 1$ in the clockwise direction (therefore violating detailed balance), with rate

$$u_\alpha(n_{i_\alpha}) = v_\alpha \frac{f_\alpha(n_{i_\alpha} - 1)}{f_\alpha(n_{i_\alpha})} \quad \text{with} \quad \alpha = 1,2, \tag{5}$$

where $f_\alpha(n_{i_\alpha})$ is a function of occupation number n_{i_α} and the factor v_α is independent of n_{i_α}. The form of the jump rates is the same as given in Eq. (5) irrespective of jumps in the bulk or jumps from one ring to the other. The factors v_α, however, can generally be different, i.e., $v_\alpha = v_\alpha^{(b)}$ when a particle jumps in the bulk of the αth ring and $v_\alpha = v_\alpha^{(c)}$ when a particle jumps in the contact region from the αth ring to the other ring. For the zero-range process, the properties of nonequilibrium steady states while two systems are in contact has been previously studied, but only for a special case when $v_\alpha^{(b)} = v_\alpha^{(c)}$ and $v_1^{(c)} = v_2^{(c)}$ [15]. Here we consider the more general case when $v_\alpha^{(b)} \neq v_\alpha^{(c)}$ as well as $v_1^{(c)} \neq v_2^{(c)}$, i.e., the factor v_α taking different values at the bulk and the contact of the two rings. However, it would be easy to see that the factor $v_\alpha^{(b)}$ taking different values in two different rings does not change the steady-state properties. Therefore, we henceforth set $v_1^{(b)} = v_2^{(b)} = 1$. In addition, for notational simplicity, we denote $v_1 \equiv v_1^{(c)}$ and $v_2 \equiv v_2^{(c)}$. For completeness, let us first discuss the special case when $v_1 = v_2$ [15]. The steady-state probability distribution can be written in a factorized form

$$P(\{n_{i_1}\},\{n_{i_2}\}) = \frac{1}{Z_N}\left[\prod_{i_1=1}^{L_1} f_1(n_{i_1}) \prod_{i_2=1}^{L_2} f_2(n_{i_2})\right] \times \delta(N_1 + N_2 - N), \tag{6}$$

where $N_1 = \sum_{i_1=1}^{L_1} n_{i_1}$ and $N_2 = \sum_{i_2=1}^{L_2} n_{i_2}$ are the numbers of particles in rings 1 and 2, respectively, and Z_N is the normalization constant. The δ function in Eq. (6) takes into account that the total number of particles $N = N_1 + N_2$ is conserved. Clearly, in this case, the joint probability distribution $P(N_1,N_2)$ of particle numbers N_1 and N_2 can be written in a product form

$$P(N_1,N_2) = \frac{Z_1(N_1)Z_2(N_2)}{Z_N}, \tag{7}$$

where $Z_\alpha(N_\alpha) = \sum_{\{n_{i_\alpha}\}} \prod_{i_\alpha=1}^{L_\alpha} f_\alpha(n_{i_\alpha}) \delta(\sum_{i_\alpha=1}^{L_\alpha} n_{i_\alpha} - N_\alpha)$. As discussed in Refs. [12,15], in this case, one can define an intensive variable $\mu_\alpha = -\partial \ln Z_\alpha / \partial N_\alpha$ that equalizes when two rings are kept in contact, i.e., $\mu_1 = \mu_2$.

Now we discuss the general case when $v_1 \neq v_2$, which leads to our main points. Interestingly, as shown in Appendix A, the steady-state probability distribution can still be written in a factorized form

$$P(\{n_{i_1}\},\{n_{i_2}\}) = \frac{1}{Z_N}\left[\prod_{i_1=1}^{L_1} f_1(n_{i_1}) \prod_{i_2=1}^{L_2} f_2(n_{i_2})\right] \times e^{\tilde{\mu}_1 N_1} e^{\tilde{\mu}_2 N_2} \delta(N_1 + N_2 - N), \tag{8}$$

where $\tilde{\mu}_1 = \ln(1/v_1)$ and $\tilde{\mu}_2 = \ln(1/v_2)$, which we call excess chemical potentials. Now the joint probability distribution $P(N_1,N_2)$ of particle numbers N_1 and N_2 can be expressed as

$$P(N_1,N_2) = \frac{Z_1(N_1)Z_2(N_2)}{Z_N} e^{\tilde{\mu}_1 N_1} e^{\tilde{\mu}_2 N_2}. \tag{9}$$

The macrostate is obtained by maximizing $\ln P(N_1,N_2)$, i.e., $\partial \ln P(N_1,N_2)/\partial N_1 = 0$. Therefore, it straightforwardly follows that

$$\left(\frac{\partial \ln Z_1}{\partial N_1} + \tilde{\mu}_1\right) = \left(\frac{\partial \ln Z_2}{\partial N_2} + \tilde{\mu}_2\right) \tag{10}$$

or, in other words, there indeed exists a new intensive variable $\mu'_\alpha = (-\partial \ln Z_\alpha / \partial N_\alpha + \ln v_\alpha)$, with $\alpha = 1,2$, which takes the same values for two rings in contact, i.e., $\mu'_1 = \mu'_2$. For the special case when $v_1 = v_2$, the excess chemical potentials are equal (i.e., $\tilde{\mu}_1 = \tilde{\mu}_2$) and drop out of Eq. (10), which then implies that the old variables μ_1 and μ_2 equalize. However, in the case when $v_1 \neq v_2$, the new variable μ'_α takes the role of the chemical potential, which then equalizes upon contact. This identification of μ'_α as an intensive variable that equalizes for two systems in contact was missed in Refs. [12,15], where it was concluded that there is no such equalization when $v_1 \neq v_2$. Moreover, contrary to the suggestion in Ref. [15], the detailed balance condition is still satisfied at the contact even when $v_1 \neq v_2$.

For a class of systems specified by a particular set of parameters $\{f_\alpha(n), v_\alpha\}$, it can be immediately checked that the zeroth law is indeed satisfied. In Fig. 13 we perform various numerical experiments similar to those discussed in

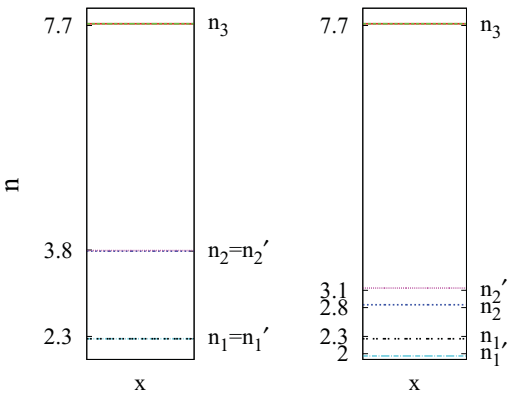

FIG. 13. (Color online) Density profiles for rings 1, 2, and 3 (all with the same size $L = 100$). The left panel shows three numerical experiments to test the zeroth law in the case of the ZRP. In experiment 1, ring 1 (with $\delta_1 = 3$ and $v_1 = 1$) is in contact with ring 3 (with $\delta_2 = 5$ and $v_2 = 0.5$). In experiment 2, ring 2 (with $\delta_1 = 4$ and $v_1 = 0.75$) is in contact with ring 3 (with $\delta_2 = 5$ and $v_2 = 0.5$). In experiment 3, ring 1 (with $\delta_1 = 3$ and $v_1 = 1$) is in contact with ring 2 (with $\delta_2 = 4$ and $v_2 = 0.75$). The zeroth law is satisfied in this case. The right panel shows three numerical experiments to illustrate the role of contact dynamics for the deviations from the zeroth law. In experiment 1, ring 1 (with $\delta_1 = 3$ and $v_1 = 1$) is in contact with ring 3 (with $\delta_2 = 5$ and $v_2 = 0.5$). In experiment 2 with slightly perturbed jump rates in the contact region, ring 2 (with $\delta_1 = 4$ and $v_1 = 0.85$) is in contact with ring 3 (with $\delta_2 = 5$ and $v_2 = 0.4$). In experiment 3, ring 1 (with $\delta_1 = 3$ and $v_1 = 1$) is in contact with ring 2 (with $\delta_2 = 4$ and $v_2 = 0.75$). The zeroth law is not satisfied in this case.

Figs. 3 and 4. We choose $f_\alpha(n) = n^{\delta_\alpha - 1}$ with various sets of parameter values for $\{\delta_\alpha, v_\alpha\}$. In the first experiment, ring 1 with $\delta_1 = 3$, $v_1 = 1$, and density $n_1 \simeq 2.3$ equilibrated with ring 3 with $\delta_2 = 5$, $v_2 = 0.5$, and density $n_3 \simeq 7.7$. In the second experiment, ring 2 with $\delta_1 = 4$, $v_1 = 0.75$, and density $n_2 \simeq 3.8$ is equilibrated with ring 3 with $\delta_2 = 5$, $v_2 = 0.5$, and density $n_3 \simeq 7.7$. In the third experiment, ring 1 with $\delta_1 = 3$, $v_1 = 1$, and density $n_1' \simeq 2.3$ is equilibrated with ring 2 with $\delta_2 = 4$, $v_2 = 0.75$, and density $n_2' \simeq 3.8$ where $n_1' \simeq n_1$ and $n_2' \simeq n_2$. In this case one can see that the zeroth law is satisfied (see the left panel of Fig. 13). We have also checked that values of the densities are such that chemical potential μ_α' takes equal values for two rings in contact. In the right panel of Fig. 13 we again perform three similar numerical experiments but now, in the second experiment, the values of the factors $v_1 = 0.85$ and $v_2 = 0.4$ are slightly perturbed by an arbitrary amount from the earlier values of the factors $v_1 = 0.75$ and $v_2 = 0.5$, which were chosen in the second experiment of the first set of numerical experiments (i.e., corresponding to the left panel of Fig. 13). One can see that, in this case, the zeroth law is violated even though the factorization property as given in Eq. (8) exactly holds in each of the three experiments. This illustrates the role of contact dynamics for the zeroth law, which is satisfied only for a precise set of jump rates in the contact region with no arbitrariness allowed in these rates.

B. Excess chemical potential in the equilibrium KLS model

The above situation in the case of the ZRP is very similar to the special case of the equilibrium KLS model when one chooses the transition rates as given in Eqs. (2) and (3) with no driving in the bulk of the individual systems, i.e., $E_1 = E_2 = 0$, and a slightly modified transition rate in the contact region as follows. In general, the transition rate for a particle jumping from system 1 to system 2 is given by

$$w(C \to C') = v_1 \min\{1, e^{-\Delta(0)}\} \tag{11}$$

and the reverse transition rate for the particle jumping from system 2 to system 1 is given by

$$w(C' \to C) = v_2 \min\{1, e^{-\Delta(0)}\}, \tag{12}$$

where we set $\beta = 1$. For $v_1 = v_2 = 1$, the jump rates in the contact region are same as given in Eq. (3). Clearly, the modified transition rates in the contact region amount to an additional field $E_{12} = \ln(v_1/v_2)$, say, from system 1 to system 2, along the bonds connecting the two systems. Note that the field E_{12} is not a driving field and just introduces an extra overall shift in the chemical potential of system 1. The field E_{12} accordingly modifies the energy function from H to H' by introducing an extra chemical potential in Eq. (1), i.e., $H' = H + E_{12}N_1$. In this case, the detailed balance is satisfied with respect to the Boltzmann distribution with the modified energy function H'. Consequently, one could effectively think of an excess contribution to the equilibrium free energy of system 1 due to the shift in the chemical potential of system 1 by an amount E_{12}. Now the condition of minimization of the total free energy $F = F_1 + F_2$, as given in Eq. (10) for the zero-range process, would imply that the new intensive variables $\mu_\alpha' = (-\partial \ln Z_\alpha/\partial N_\alpha + \ln v_\alpha)$, not the variables $\mu_\alpha = -\partial \ln Z_\alpha/\partial N_\alpha$, equalize where the free energies of the respective systems are $F_1 = -\ln Z_1 + \tilde{\mu}_1 N_1$ and $F_2 = -\ln Z_2 + \tilde{\mu}_2 N_2$ with partition function $Z_\alpha = \sum_C e^{-H_\alpha(C)}$, the energy function for the individual systems $H_\alpha = K_\alpha \sum_{\langle \mathbf{r}_\alpha, \mathbf{r}_\alpha' \rangle} \eta(\mathbf{r}_\alpha)\eta(\mathbf{r}_\alpha')$ [see Eq. (1)] for $\alpha = 1,2$. Consequently, the zeroth law is satisfied in the case when each system is assigned a particular set of values of the factors v_α. However, if the factors v_α are chosen arbitrarily in any of the numerical experiments as shown in the right panel of Fig. 13 in the case of the ZRP, the zeroth law would not hold even for the equilibrium KLS model with the modified jump rates in the contact region.

V. ANALYTICAL APPROACHES FOR THE DRIVEN KLS MODEL

In this section we discuss first how the zeroth law, which has been shown to be satisfied to a very good approximation in the simulations of the driven KLS model for various parameter values, could be explained in terms of the large-deviation principle. Then we discuss how the deviations from the zeroth law, also observed in the simulations, could be explained by modifying this large-deviation principle.

A. Large-deviation principle

In equilibrium, the zeroth law can be derived from variational principles, e.g., by maximization of entropy of an isolated system or by minimization of free energy in the case in which the system is in contact with a reservoir. For some nonequilibrium systems, there may be a similar principle, called the large-deviation principle [3,26]. The zeroth law can be derived from the large-deviation principle along the same lines as in equilibrium in the following way. Let us consider the scenario in which two systems are kept in contact with each other with a particular dynamics specified in the contact region. The two systems exchange, according to the contact dynamics, some conserved quantity, say, the number of particles, such that $N_1 + N_2 = N = \text{const}$, with N_1 and N_2 the number of particles in systems 1 and 2, respectively (schematically shown in Fig. 1). The quantities N_1 and N_2 are considered to be extensive, i.e., proportional to the volumes V_1 and V_2 of systems 1 and 2, respectively. We are interested in large deviations of N_1 and N_2 and assume that the probability of a large deviation $P(N_1, N_2)$ in the quantities N_1 and N_2 is given by

$$P(N_1, N_2) \sim \frac{e^{-V_1 f_1(n_1)} e^{-V_2 f_2(n_2)}}{e^{-F(N)}} \tag{13}$$

in the limit of $N_1, N_2, V_1, V_2 \gg 1$, keeping their respective densities $n_1 = N_1/V_1$ and $n_2 = N_2/V_2$ finite with the normalization constant $\exp[-F(N)]$. Equation (13) is the statement of the large-deviation principle [3,26] and the functions $f_1(n_1)$ and $f_2(n_2)$ are called the large-deviation functions for the corresponding systems. The sign "$\sim$" implies equality in terms of the logarithm of the respective quantities and Eq. (13) can be written more rigorously as

$$-\ln P(N_1, N_2) = V_1 f_1(n_1) + V_2 f_2(n_2) - F(N) + \epsilon(N_1, N_2), \tag{14}$$

where $\epsilon(N_1, N_2)/\ln P(N_1, N_2) \to 0$ as $N_1, N_2 \to \infty$. Note that in writing Eqs. (13) and (14) we have assumed that the

correlation between systems 1 and 2 can be neglected as a boundary effect in the limit of large volume. To ensure that the correlation is minimal, in this paper we consider the model of two systems in contact where the contact area is chosen to be very small compared to the volume of each of the systems so that the contact region does not affect the bulk of the systems much. In the case in which the contact area is comparable to the volume of the system, as in the case of driven bilayer systems studied before [24], the combined system may not be divided into two subsystems and in that case the fluctuations in the subsystems are not independent of each other.

Now, from Eq. (14), the macroscopic stationary state $\{N_1^*, N_2^*\}$, under the constraint $N_1 + N_2 = \text{const}$, can be determined by maximizing $\ln P(N_1, N_2)$, i.e., $\partial \ln P(N_1, N_2)/\partial N_1 = 0$, which gives

$$\left(\frac{\partial f_1}{\partial n_1}\right)_{n_1^*} = \left(\frac{\partial f_2}{\partial n_2}\right)_{n_2^*} = \mu, \tag{15}$$

where $n_1^* = N_1^*/V_1$, $n_2^* = N_2^*/V_2$, and μ is the chemical potential, which takes the same values in the steady state when systems 1 and 2 are kept in contact. Note that the validity of Eq. (15), which implies the existence of an intensive thermodynamic variable, follows from the assumption of the large-deviation principle of Eq. (13). The preceding arguments are quite general and could be valid irrespective of the specific nature of the dynamics one considers in a particular problem. Therefore, Eq. (15) can be equally applicable to an equilibrium and a nonequilibrium steady state. Another consequence of equalization of intensive variables is the fluctuation-response relation between the compressibility and the fluctuations in particle number N_1 of system 1, i.e.,

$$\frac{\partial \langle N_1 \rangle}{\partial \mu} = \langle N_1^2 \rangle - \langle N_1 \rangle^2, \tag{16}$$

when system 1 is kept in contact with a very large system 2, with chemical potential μ, which can be considered as a particle reservoir (i.e., $N_1 \ll N_2$ and $V_1 \ll V_2$). For more details regarding the above fluctuation relation in the context of the ZRP as well as for the KLS model, see Appendix B.

B. Modified large-deviation principle

The exact results for the ZRP and the equilibrium KLS model give us insight into the role of the contact dynamics, which can effectively introduce an excess chemical potential across the contact region. Consequently, the intensive variable for a system that equalizes upon contact can have different functional forms depending on the specifics of the dynamics in the contact region and therefore on the other system in contact. To describe this situation in a more general context where there may be equalization of an intensive variable but still the zeroth law does not strictly hold, we write the large-deviation probabilities as given in Eq. (13) in a modified asymptotic form

$$P(N_1, N_2) \sim \frac{e^{-V_1 f_1(n_1)} e^{-V_2 f_2(n_2)} e^{\tilde{\mu}_1 N_1} e^{\tilde{\mu}_2 N_2}}{e^{-F(N)}} \tag{17}$$

where f_1 and f_2 are the large-deviation functions for a putative contact dynamics for which the zeroth law is satisfied and the two additional quantities $\tilde{\mu}_1$ and $\tilde{\mu}_2$ can be thought of as excess chemical potentials arising solely due to the actual contact dynamics that is under consideration for which the zeroth law is not satisfied. Clearly, for an arbitrarily chosen contact dynamics, the old intensive variables $\mu_1 = \partial f_1/\partial n_1$ and $\mu_2 = \partial f_2/\partial n_2$ do not equalize. Note that, unlike in the case of the ZRP or the equilibrium KLS model, the potentials $\tilde{\mu}_1$ and $\tilde{\mu}_2$ generally are *a priori* unknown for a given contact dynamics. Moreover, for an arbitrarily chosen contact dynamics, it may not always be possible to assign to the individual systems an intensive variable that is independent of the specifics in the contact region between two systems. In this case, even though there can be equalization of some intensive variable when two systems are kept in contact, the zeroth law may not be satisfied as demonstrated in the case of the ZRP (see the right panel of Fig. 13).

The modified large-deviation principle in Eq. (17) still assumes that two systems in contact have an asymptotic factorization property in the sense that the correlations between the systems can be ignored in the large-volume limit. In a special case (e.g., the ZRP or the equilibrium KLS model), the chemical potentials $\tilde{\mu}_1$ and $\tilde{\mu}_2$ can be constant over an entire density range. However, in general, the quantities $\tilde{\mu}_1(n_1)$ and $\tilde{\mu}_2(n_2)$ can be functions of densities n_1 and n_2. Note that, although the large-deviation principles in Eqs. (13) and (17) appear to have different forms, they are essentially the same. The only difference is that in the modified form of Eq. (17) we identify the contribution to the large-deviation function due to the contact dynamics and separate this contribution from that arising due to the bulk of the individual systems.

The asymptotic factorization can indeed be a very good approximation even in the case of a more complicated driven lattice gas such as the KLS model. To show this we now study various spatial density correlations $c_{ij}^{(\alpha)}(r_{j,\alpha})$ between two points located in the individual systems as well as two points located in two different systems across the contact region. We define the function

$$c_{ij}^{(\alpha)}(r_{j,\alpha}) = \frac{\langle \{\Delta\eta(\mathbf{r}_i^c)\}\{\Delta\eta(\mathbf{r}_j^c + \mathbf{r}_j)\}\rangle}{\sqrt{\langle \{\Delta\eta(\mathbf{r}_i^c)\}^2\rangle}\sqrt{\langle \{\Delta\eta(\mathbf{r}_j^c + \mathbf{r}_j)\}^2\rangle}}, \tag{18}$$

which denotes the scaled correlation along αth direction between two points in systems i and j, where $r_{j,\alpha}$ is the αth component of the position vector $\mathbf{r}_j$ with $i, j = 1,2$ and $\alpha = x, y$ (for a two-dimensional system), $\Delta\eta(\mathbf{r}) = \eta(\mathbf{r}) - \langle\eta(\mathbf{r})\rangle$ is the fluctuation in the occupation variable $\eta(\mathbf{r})$, and $\mathbf{r}_i^c$ is the position vector of the contact site in system i. For $i = j$, $c_{ii}^{(\alpha)}(r_{i,\alpha})$ denotes the density correlation, along the α axis, between two points, both located in the same system i and, for $i \neq j$, $c_{ij}^{(\alpha)}(r_{j,\alpha})$ denotes the cross correlation, along the α axis, between two points, one located in system i and the other located in system j. In Fig. 14 the scaled correlation $c_{ij}^{(\alpha)}(r_{j,\alpha})$ is plotted as a function of $r_{j,\alpha}$ for a driven system with $K_1 = -0.75$, $E_1 = 4$, and an equilibrium system with $K_2 = -0.75$, where the systems are kept in contact, both at density $n = 1/2$. One can see that the amplitude of the cross correlations among nearest-neighbor sites located in two different systems across the contact region are very small, almost an order of magnitude smaller than those among neighboring sites in the individual systems, i.e., $c_{21}^{(\alpha)}(0), c_{12}^{(\alpha)}(0) \ll c_{11}^{(\alpha)}(1), c_{22}^{(\alpha)}(1)$.

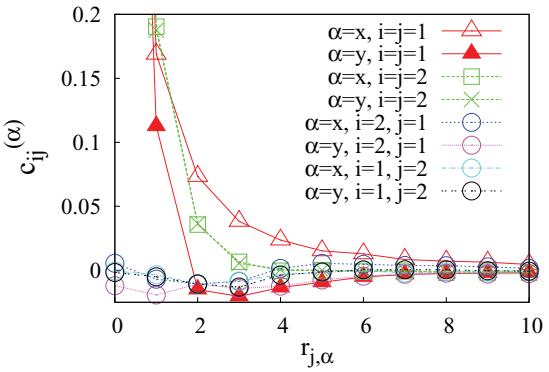

FIG. 14. (Color online) Correlations between various neighboring sites as a function of distance when a driven system 1 (with $K = -0.75$, $E = 4$, and $V = 50 \times 50$) and an equilibrium system 2 (with $K = -0.75$, $E = 0$, and $V = 50 \times 50$) are in contact (in the 2×2 contact region) with each other. The function $c_{ij}^{(\alpha)}(r_{j,\alpha})$ denotes the scaled correlation [see Eq. (18)] in the αth direction between two points located in systems i and j, where $r_{j,\alpha}$ is the αth component of the relative position vector $\mathbf{r}_j$ between the two points with $i, j = 1,2$ and $\alpha = x, y$ (for two-dimensional systems), and $\Delta\eta(\mathbf{r}) = \eta(\mathbf{r}) - \langle\eta(\mathbf{r})\rangle$ is the fluctuation in the occupation variable $\eta(\mathbf{r})$. For $i \neq j$, $c_{ij}^{(\alpha)}(r_{j,\alpha} = 0)$ is the correlation between two nearest-neighbor sites located across the contact.

Therefore, the asymptotic factorization property is expected to be well satisfied in this case. Moreover, the very weak cross correlation between two systems in contact explains why the density profiles remain almost homogeneous even around the contact. Note that the density-correlation functions $c_{11}^{(x)}(r_{1,x})$ and $c_{11}^{(y)}(r_{1,y})$ for the driven system in the x and y directions, respectively, are clearly different due to the presence of a strong driving field that breaks the isotropy, whereas for the equilibrium system the correlations $c_{22}^{(x)}(r_{1,x})$ and $c_{22}^{(y)}(r_{1,y})$ remain the same, as expected. For attractive interaction strengths, the correlations perpendicular to the driving field become negative at larger distances. This picture remains qualitatively the same at other densities as well.

C. Excess chemical potential in the driven KLS model

The role of the contact dynamics in the KLS model can be more complex than that in the previously discussed models of the ZRP. However, interestingly for some parameter values, we indeed find evidence of a constant difference $\delta\mu = \tilde{\mu}_1 - \tilde{\mu}_2$ in the excess chemical potentials in a wide density range even in the KLS model for nonzero driving. This supports the modified form of the large-deviation principle even for the KLS model.

We consider the density n as a function of the chemical potential μ for a driven system with $K = -1$ and $E = 6$ that is separately kept in contact with various equilibrium systems with interaction strengths $K = 0$, -0.8, and -0.9. As we have already shown in Fig. 11 for the same systems, there were indeed deviations from the zeroth law observed as the different curves for n vs μ in Fig. 11 do not fall on each other. However, by now shifting the chemical potential μ to $\mu + \delta\mu$ and choosing a suitable $\delta\mu$ in each of the cases, all the curves can be made to collapse on each other quite well, as can be seen in Fig. 15.

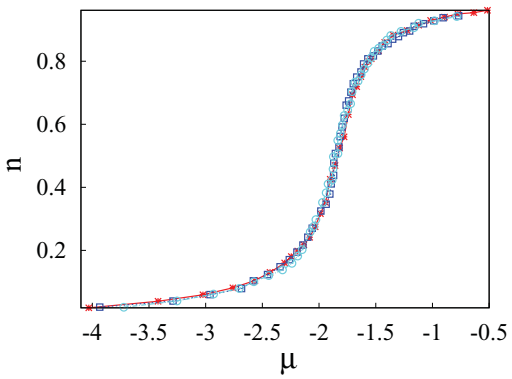

FIG. 15. (Color online) Density n vs shifted chemical potential μ plotted for a driven system with $K = -1$ and $E = 6$, which is separately kept in contact (in the 2×2 contact region) with three equilibrium systems with interaction strengths $K = 0$, -0.8, and -0.9. By shifting $\mu \to \mu + \delta\mu$, all curves collapse on each other well where we choose $\delta\mu = 0.06$ and 0.095 for the cases in which the driven system is in contact with the equilibrium systems with $K = -0.8$ and -0.9, respectively.

We have done the same analysis for another driven system with a different set of parameter values $K = 3.75$ and $E = 6$. The driven system is separately kept in contact with two equilibrium systems with interaction strengths $K = 0.75$ and 1.0. In Fig. 16 the densities n are plotted as a function of the shifted chemical potential μ (also see Fig. 12). The curves could be collapsed on top of each other reasonably well by shifting the μ to $\mu + \delta\mu$.

However, for both cases in Figs. 15 and 16, it should be noted that the collapse is not so good at very low chemical potentials (i.e., low densities). This indicates that the difference in the excess chemical potential $\delta\mu$ actually may not be constant over the entire chemical potential range and can depend on the chemical potential itself (or, equivalently, the density) of the corresponding equilibrium system in contact.

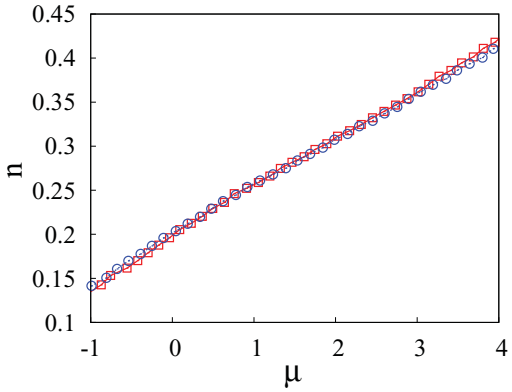

FIG. 16. (Color online) Density n vs shifted chemical potential μ plotted for a driven system with $K = 3.75$ and $E = 6$, which is separately kept in contact (in the 2×2 contact region) with two equilibrium systems with $K = 0.75$ and 1. Shifting $\mu \to \mu + \delta\mu$, two curves collapse on each other reasonably well by choosing $\delta\mu = 0.1$ for the case when the driven system is in contact with the equilibrium system with $K = 0.75$.

VI. CONCLUDING PERSPECTIVE

In this paper we have studied equilibration of driven lattice gases when two systems are kept in contact and allowed to exchange particles with the total number of particles conserved. Interestingly, for both attractive and repulsive nearest-neighbor interactions and for a wide range of parameter values, there is a remarkably simple, though approximate, thermodynamic structure where the zeroth law is quite well satisfied.

However, deviations from this simple thermodynamic law are also observed. To understand these deviations, we studied the nontrivial role of the contact dynamics for a variant of the zero-range process as well as a variant of the equilibrium Katz-Lebowitz-Spohn model, where one can calculate the steady-state probability distribution exactly. Using these simple examples, we pointed out that, due to the modified contact dynamics, there can be an excess chemical potential induced across the contact region. These results led us to express the large-deviation principle in a modified form that elucidates the role of the contact and can substantially account for the deviations from the zeroth law.

It is important to note that the modified form of the large-deviation principle is still based on the asymptotically factorized form of the steady-state distribution for two driven systems in contact and is valid if the correlations between the systems can be neglected in the large-volume limit. In the case of the variant of the ZRP discussed here, these correlations are zero. In the case of the driven KLS model, we observed that the spatial density correlations across the contact are indeed very small compared to the nearest-neighbor correlations in the individual systems. Interestingly, we found evidence of an almost constant excess chemical potential for various parameter values and in a wide range of densities, therefore supporting the applicability of the modified large-deviation principle to the KLS model.

In general, the results in this paper lead us roughly to the following possible scenarios for driven systems in contact.

(i) The large-deviation principle (in other words, the asymptotic factorization property) may break down due to long-ranged correlations that may be present in the driven systems [27–29]. In this case, the combined system cannot be divided into independent subsystems and there would be no intensive variable that equalizes upon contact.

(ii) However, when the amplitudes of these correlations are sufficiently weak, it is possible that a large-deviation principle holds, although in a modified form. In these cases, the systems can be characterized by the excess chemical potentials across the contact and consequently there would be some intensive variable that would then equalize upon contact. Note that introducing the excess chemical potential is essentially a way of reparametrization of the chemical potential of the driven system under consideration. These excess chemical potentials can depend on the specifics of the contact dynamics and they are generally *a priori* unknown, therefore in a sense arbitrary. For some parameter values, the excess chemical potential may be almost constant over a range of densities. In special cases, the arbitrariness of the excess chemical potential can be removed by choosing a suitable contact dynamics such that the zeroth law strictly holds. In these cases it is actually possible to assign to the individual systems an intensive variable, independent of the specifics in the contact region between two systems, which would then equalize. It should be noted here that the modified large-deviation principle could be satisfied irrespective of whether or not the zeroth law is satisfied, which has been illustrated in this paper by using a variant of the ZRP.

For the ZRP, since the steady-state properties are exactly known, it is easier to choose a contact dynamics so that the zeroth law can be satisfied. However, for the KLS model that has nontrivial steady-state properties, it would be difficult to find a contact dynamics, even if it exists, for which the zeroth law would strictly hold. For the KLS model, here we have considered a contact dynamics, mainly based on a physical ground albeit on an *ad hoc* basis, that satisfies the local detailed balance condition. The simple modification of the large-deviation principle suggested in this paper indicates that it could still be possible to choose a contact dynamics such that the thermodynamic laws are satisfied even better. The origin of the excess chemical potential in the contact region should be understood in more detail, which could give valuable insight into whether it is possible to choose a contact dynamics for which a simple thermodynamic structure emerges for driven systems in general.

There are additional important aspects in exploring such a simple structure for driven systems in contact. Unlike in equilibrium, where there is a well-defined prescription to describe various thermodynamic properties using the standard Boltzmann distribution, there is no such prescription for nonequilibrium systems. However, the numerically observed simple thermodynamic structure concerning driven lattice gases in contact may give us a useful tool to characterize such systems and offers the possibility of describing phase transitions that are known to occur in these driven interacting many-particle systems.

ACKNOWLEDGMENT

We thank R. K. P. Zia for stimulating discussions.

APPENDIX A: STEADY-STATE DISTRIBUTION FOR THE ZRP WHEN $v_1 \neq v_2$

In the general case when $v_1 \equiv v_1^{(c)} \neq v_2 \equiv v_2^{(c)}$, the ansatz for the steady-state probability distribution is given by

$$P_{\rm st}(\{n_{i_1}\},\{n_{i_2}\}) = \frac{1}{Z_N}\left[\prod_{i_1=1}^{L_1} f_1(n_{i_1}) \prod_{i_2=1}^{L_2} f_2(n_{i_2})\right] \times \frac{1}{v_1^{N_1} v_2^{N_2}} \delta(N_1 + N_2 - N), \qquad \text{(A1)}$$

where N_1 and N_2 are the numbers of particles in rings 1 and 2, respectively, and $N = N_1 + N_2$ is the total conserved particle number. Now we consider the two following cases: (i) when a particle jumps in the bulk, say, in ring 1, and (ii) when a particle jumps from one ring to the other.

Case (i). Consider the two following transitions from a configuration C to C' and a configuration C'' to C where $C \equiv (\{\ldots,n_{i_1-1},n_{i_1},n_{i_1+1},\ldots\},\{n_{i_2}\})$, $C' \equiv (\{\ldots,n_{i_1-1},n_{i_1}-1,n_{i_1+1}+1,\ldots\},\{n_{i_2}\})$, and $C'' \equiv (\{\ldots,n_{i_1-1}+1,n_{i_1}-1,n_{i_1+1},\ldots\},\{n_{i_2}\})$. The steady-state probability current $J(C \to C') = P_{\rm st}(C)w(C'|C)$ from

configuration C to C' [where $P_{\rm st}(C)$ is the probability of configuration C in a steady state and $w(C'|C)$ is the transition rate from C to C'] can be explicitly written as

$$J(C\to C') = \frac{1}{Z_N}[\cdots f(n_{i_1-1})f(n_{i_1})f(n_{i_1+1})\cdots] \times \left[v_1^{(b)}\frac{f(n_{i_1}-1)}{f(n_{i_1})}\right]\left[\prod_{i_2=1}^{L_2} f_2(n_{i_2})\right] \times \frac{1}{v_1^{N_1}v_2^{N_2}}\delta(N_1+N_2-N), \tag{A2}$$

where we have used the jump rate in the bulk of ring 1, which is $w(C'|C) = v_1^{(b)} f(n_{i_1}-1)/f(n_{i_1})$. Finally, we get

$$J(C\to C') = \frac{1}{Z_N}[\cdots f(n_{i_1-1})f(n_{i_1}-1)f(n_{i_1+1})\cdots] \times \left[\prod_{i_2=1}^{L_2} f_2(n_{i_2})\right]\frac{v_1^{(b)}}{v_1^{N_1}v_2^{N_2}}\delta(N_1+N_2-N). \tag{A3}$$

Similarly, the probability current $J(C''\to C) = P(C'')w(C|C'')$ from configuration C'' to C can be explicitly written as

$$\begin{aligned} J(C''\to C) &= \frac{1}{Z_N}[\cdots f(n_{i_1-1}+1)f(n_{i_1}-1)f(n_{i_1+1})\cdots] \times \left[v_1^{(b)}\frac{f(n_{i_1-1})}{f(n_{i_1-1}+1)}\right]\left[\prod_{i_2=1}^{L_2} f_2(n_{i_2})\right] \times \frac{1}{v_1^{N_1}v_2^{N_2}}\delta(N_1+N_2-N) \\ &= \frac{1}{Z_N}[\cdots f(n_{i_1-1})f(n_{i_1}-1)f(n_{i_1+1})\cdots] \times \left[\prod_{i_2=1}^{L_2} f_2(n_{i_2})\right]\frac{v_1^{(b)}}{v_1^{N_1}v_2^{N_2}}\delta(N_1+N_2-N). \end{aligned} \tag{A4}$$

The probability currents $J(C\to C')$ and $J(C''\to C)$ are clearly equal. Since for any transition from C to C' it is always possible to find a corresponding transition C'' to C, the net current into C vanishes pairwise, i.e., $J(C\to C') = J(C''\to C)$ in the steady state.

Case (ii). Consider two transitions from C to C' and the configuration C' to C where $C \equiv (\{\ldots,n_{k_1},\ldots\},\{\ldots,n_{k_2},\ldots\})$, $C' \equiv (\{\ldots,n_{k_1}-1,\ldots\},\{\ldots,n_{k_2}+1,\ldots\})$, and k_1 and k_2 are the respective contact sites in rings 1 and 2. In this case the probability current $J(C\to C')$ can be written as

$$\begin{aligned} J(C\to C') &= \frac{1}{Z_N}[\cdots f(n_{k_1})\cdots]\left[v_1\frac{f(n_{k_1}-1)}{f(n_{k_1})}\right] \times [\cdots f(n_{k_2})\cdots]\frac{1}{v_1^{N_1}v_2^{N_2}}\delta(N_1+N_2-N) \\ &= \frac{1}{Z_N}[\cdots f(n_{k_1}-1)\cdots][\cdots f(n_{k_2})\cdots] \times \frac{1}{v_1^{N_1-1}v_2^{N_2}}\delta(N_1+N_2-N) \end{aligned} \tag{A5}$$

Similarly, the probability current $J(C'\to C)$ can be written as

$$\begin{aligned} J(C'\to C) &= \frac{1}{Z_N}[\cdots f(n_{k_1}-1)\cdots][\cdots f(n_{k_2}+1)\cdots] \times \left[v_2\frac{f(n_{k_2})}{f(n_{k_2}+1)}\right]\frac{1}{v_1^{N_1-1}v_2^{N_2+1}}\delta(N_1+N_2-N) \\ &= \frac{1}{Z_N}[\cdots f(n_{k_1}-1)\cdots][\cdots f(n_{k_2})\cdots] \times \frac{1}{v_1^{N_1-1}v_2^{N_2}}\delta(N_1+N_2-N). \end{aligned} \tag{A6}$$

Clearly, the net probability current into C is again zero as $J(C\to C') = J(C'\to C)$ in the steady state. This completes the proof for the steady-state ansatz given in Eq. (A1), which satisfies master equation $\partial_t P_{\rm st}(C,t) = 0 = \sum_{C'\neq C}[P_{\rm st}(C')w(C'\to C) - P_{\rm st}(C)w(C\to C')]$. Note that the condition $J(C\to C') = J(C'\to C)$ is nothing but the detailed balance condition that is satisfied in the contact region even when $v_1 \neq v_2$. However, detailed balance is not satisfied in the bulk and consequently there are nonzero currents within the individual systems.

APPENDIX B: FLUCTUATION-RESPONSE RELATIONS

One interesting consequence of Eq. (15) is a relation between the susceptibility and the fluctuation in particle number of a system when the system is in contact with a large reservoir characterized by a chemical potential μ. Consider that system 1 is in contact with system 2, which is very large compared to system 1. Let us denote by $\sigma^2_{N_1}$ the standard deviation of fluctuations in the total number of particles N_1 in system 1, i.e., $\sigma^2_{N_1} = \langle N_1^2\rangle - \langle N_1\rangle^2$. Then the large-deviation principle with the definition of chemical potential as given in Eq. (15) implies that the fluctuation of particle number around an average particle number N_1^*,

$$P(N_1) \approx {\rm const}e^{-(N_1-N_1^*)^2/2\chi}, \tag{B1}$$

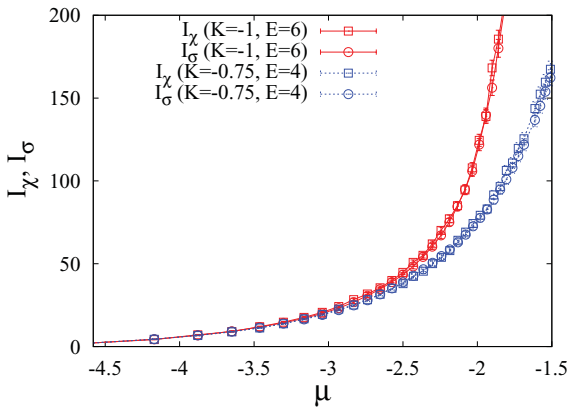

FIG. 17. (Color online) A 20×20 driven system in contact (in the 2×2 contact region) with a 250×250 equilibrium reservoir of noninteracting hard-core particles. Integrated compressibility I_χ (squares) and integrated fluctuation I_σ (circles) plotted as a function of μ for a driven system with two different sets of parameter values with $K=-1$ and $E=6$ (solid red line) and with $K=-0.75$ and $E=4$ (dotted blue line). The fluctuation-response relation is well satisfied.

where $1/\chi = \partial\mu/\partial N_1 = (\partial^2 F_1/\partial N_1^2)_{N_1^*}$ with $F_1(N_1) = V_1 f_1(n_1)$. Since the root-mean-square fluctuation in the particle number N_1 is $\sigma_{N_1}^2 = 2\chi$, one gets the fluctuation relation

$$\frac{\partial\langle N_1\rangle}{\partial\mu} = \left(\langle N_1^2\rangle - \langle N_1\rangle^2\right). \tag{B2}$$

For the ZRP, even when $v_1 \neq v_2$, the fluctuation-response relation between the compressibility and the root-mean-square fluctuation in particle number N_1 is still exactly satisfied if ring 1 is in contact with a much larger ring 2, which is a particle reservoir. Moreover, since in this case the variables μ'_α and μ_α differ only by a constant $\ln v_\alpha$ [see Eq. (10) and the text immediately following it], the fluctuation-response relation is satisfied with respect to both the new and old intensive variables μ'_α and μ_α, respectively.

Now we briefly discuss the numerical results concerning the fluctuation-response relation for the KLS model with attractive interaction strengths. To numerically test the fluctuation relation as given in Eq. (B2), we consider a driven system that is in contact with an equilibrium reservoir of hard-core particles that are otherwise noninteracting (i.e., $K = 0$). The chemical potential μ of the equilibrium hard-core particle reservoir is given by the expression in Eq. (4). For better numerical accuracy, we check the integrated version of Eq. (B2), i.e., we calculate the integrated fluctuation $I_\sigma = \int_{\mu_0}^{\mu}(\sigma_{N_1}^2)d\mu'$ and the integrated susceptibility $I_\chi = \int_{\mu_0}^{\mu}(d\langle N_1\rangle/d\mu')d\mu'$ for different values of μ obtained by varying the density of the equilibrium reservoir. We take a two-dimensional 20×20 nonequilibrium system in contact with a 250×250 equilibrium reservoir. In Fig. 17 the integrated compressibility and the integrated fluctuations are plotted as a function of chemical potential μ for two driven systems with two different sets of parameter values with $K = -1$ and $E = 6$ and with $K = -0.75$ and $E = 4$. In these cases, the fluctuation-response relation is remarkably well satisfied, as seen in Fig. 17.

[1] J. Marro and R. Dickman, *Nonequilibrium Phase Transitions in Lattice Models* (Cambridge University Press, Cambridge, 2005).
[2] R. K. P. Zia and B. Schmittmann, J. Stat. Mech. (2007) P07012.
[3] G. L. Eyink, J. L. Lebowitz, and H. Spohn, J. Stat. Phys. **83**, 385 (1996).
[4] Y. Oono and M. Paniconi, Prog. Theor. Phys. Suppl. **130**, 29 (1998).
[5] L. Bertini, A. De Sole, D. Gabrielli, G. Jona-Lasinio, and C. Landim, Phys. Rev. Lett. **87**, 040601 (2001); J. Stat. Phys. **107**, 635 (2002).
[6] T. Bodineau and B. Derrida, Phys. Rev. Lett. **92**, 180601 (2004).
[7] S. Sasa and H. Tasaki, J. Stat. Phys. **125**, 125 (2006).
[8] H.-Q. Wang and N. Menon, Phys. Rev. Lett. **100**, 158001 (2008).
[9] S. Henkes, C. S. O'Hern, and B. Chakraborty, Phys. Rev. Lett. **99**, 038002 (2007).
[10] Y. Shokef, G. Shulkind, and D. Levine, Phys. Rev. E **76**, 030101(R) (2007).
[11] K. Hayashi and S. Sasa, Phys. Rev. E **68**, 035104 (2003).
[12] E. Bertin, O. Dauchot, and M. Droz, Phys. Rev. Lett. **96**, 120601 (2006).
[13] M. R. Evans and T. Hanney, J. Phys. A **38**, R195 (2005).
[14] S. N. Majumdar, M. R. Evans, and R. K. P. Zia, Phys. Rev. Lett. **94**, 180601 (2005); M. R. Evans, T. Hanney, and S. N. Majumdar, *ibid.* **97**, 010602 (2006).
[15] E. Bertin, K. Martens, O. Dauchot, and M. Droz, Phys. Rev. E **75**, 031120 (2007).
[16] S. Katz *et al.*, J. Stat. Phys. **34**, 497 (1984); S. Katz, J. L. Lebowitz, and H. Spohn, *ibid.* **34**, 497 (1984).
[17] B. Schmittmann and R. K. P. Zia, Phys. Rep. **301**, 45 (1998); R. K. P. Zia, J. Stat. Phys. **138**, 20 (2010).
[18] W. Dietrich, P. Fulde, and I. Peschel, Adv. Phys. **29**, 527 (1980).
[19] J. Marro, J. L. Lebowitz, H. Spohn, and M. H. Kalos, J. Stat. Phys. **38**, 725 (1985); J. L. Valles and J. Marro, *ibid.* **43**, 441 (1986); **49**, 89 (1987); K.-t. Leung, Phys. Rev. Lett. **66**, 453 (1991); J.-S. Wang, J. Stat. Phys. **82**, 1409 (1996).
[20] K.-t. Leung, B. Schmittmann, and R. K. P. Zia, Phys. Rev. Lett. **62**, 1772 (1989).
[21] R. Dickman, Phys. Rev. A **38**, 2588 (1988); **41**, 2192 (1990); P. L. Garrido, J. Marro, and R. Dickman, Ann. Phys. (NY) **199**, 366 (1990).
[22] H. K. Janssen and B. Schmittmann, Z. Phys. B **64**, 503 (1986); K.-t. Leung and J. L. Cardy, J. Stat. Phys. **44**, 567 (1986); A. Achahbar, P. L. Garrido, J. Marro, and M. A. Muñoz, Phys. Rev. Lett. **87**, 195702 (2001); M. A. Muñoz, in *Nonequilibrium Statsitical Physics Today*, edited by P. L. Garrido, J. Marro, and F. de los Santos, AIP Conf. Proc. No. 1332 (AIP, New York, 2011), p. 111.
[23] P. Pradhan, C. P. Amann, and U. Seifert, Phys. Rev. Lett. **105**, 150601 (2010).
[24] A. Achahbar and J. Marro, J. Stat. Phys. **78**, 1493 (1995); C. C. Hill, R. K. P. Zia, and B. Schmittmann, Phys. Rev. Lett. **77**, 514 (1996).
[25] A. Achahbar, P. L. Garrido, and J. Marro, Mol. Phys. **88**, 1157 (1996).
[26] H. Touchette, Phys. Rep. **478**, 1 (2009).
[27] J. R. Dorfman, T. R. Kirkpatrick, and J. V. Sengers, Annu. Rev. Chem. **45**, 213 (1994).
[28] P. L. Garrido, J. L. Lebowitz, C. Maes, and H. Spohn, Phys. Rev. A **42**, 1954 (1990); **42**, 1954 (1990).
[29] G. Grinstein, D. H. Lee, and S. Sachdev, Phys. Rev. Lett. **64**, 1927 (1990).